Part III Optical Properties of Materials

12.1 Introduction

- From the classical point of view, it is not evident why the electrons should behave freely at low frequencies and respond as if they would be bound at higher frequencies.

- An unconstrained interpretation for this is only possible by applying wave mechanics. This will be done in the present chapter.
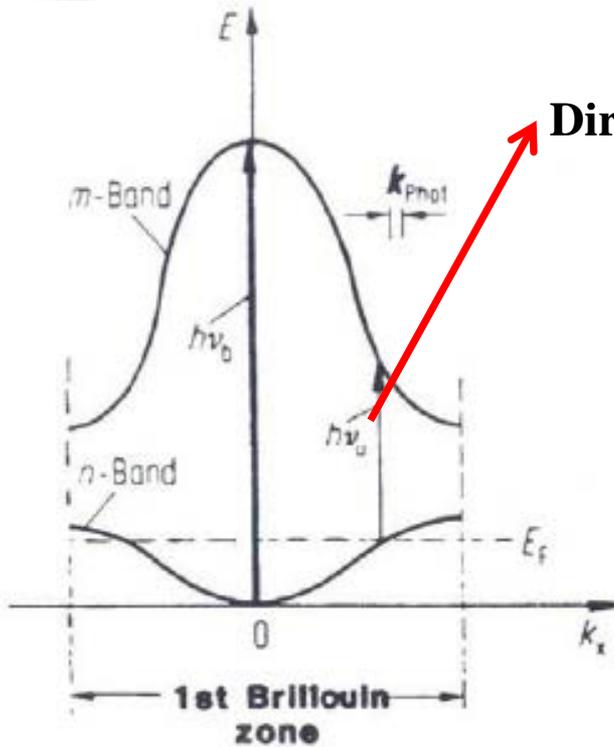
Direct interband transitions

Electron transitions at which k remains constant .

Figure 12.1. Electron bands and direct interband transitions in a reduced zone. (Compare with Fig. 5.4.)

Indirect interband transitions

It accompany phonon with properties that absorb very small energies but able to absorb a large momentum comparable to that of an electron
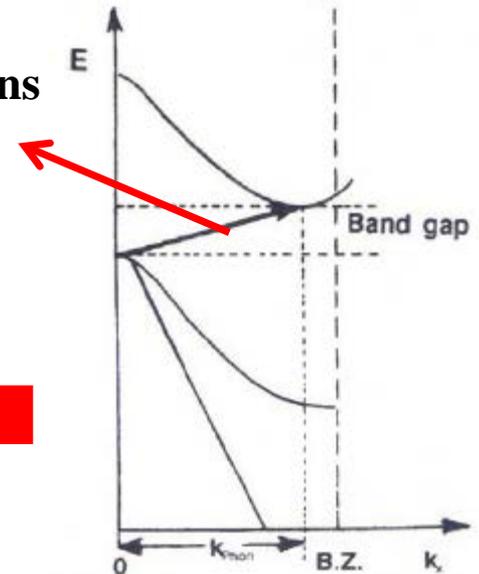
Figure 12.2. Indirect interband transition. (The properties of phonons are explained in Chapter 20.)
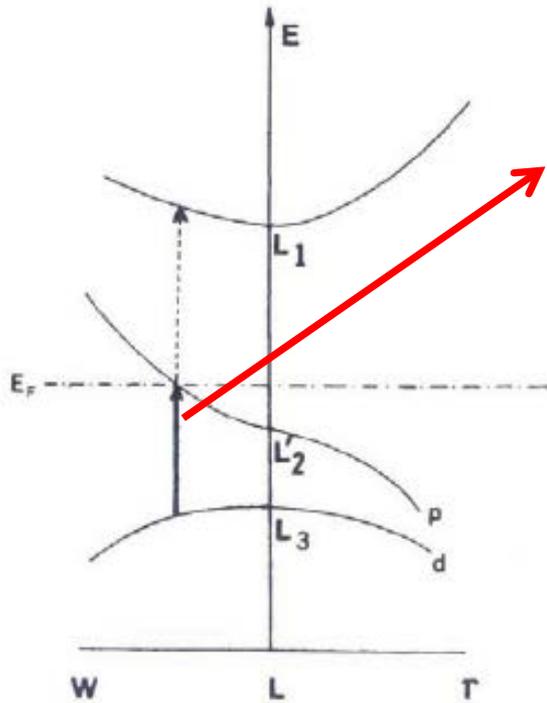
Threshold energy for interband transitions

The interband transition having the smallest possible energy difference is shown to occur between the upper d-band and the Fermi energy

Figure 12.3. Section of the band diagram for copper (schematic). Two pertinent interband transitions are shown with arrows. The smallest possible interband transition occurs from a filled d-state to an unfilled state just above the Fermi energy.

Under certain conditions photons may excite electrons into a higher energy level within the same band. This occurs with participation of a phonon, i.e. a lattice vibration quantum
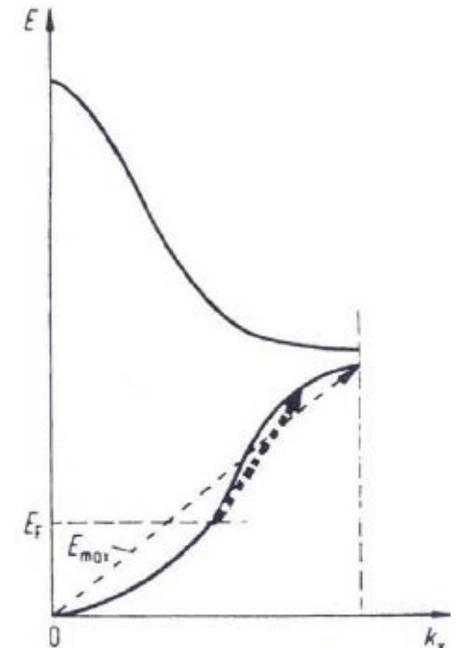
Figure 12.4. Intraband transitions. The largest energy that can be absorbed by intraband transitions is obtained by projecting the arrow marked "E_{max}" onto the energy axis.

12.3 Optical Spectra of Materials

- Optical spectra are the principal means to obtain experimentally the band gap and energies for interband transition.

- For isolated atoms and ions, the absorption and emission spectra are known to be extremely sharp.

- Plain reflection spectra of solids are not to useful for deduction of transition energies, mainly because R is a rather involved function of ε_1 and ε_2 : Thus ε_2 (i.e. absorption) spectra are often utilized instead.

- Modulated optical spectra (Sec 13.1.3) separate the small contributions stemming from points of high symmetry (such as the centers and edges of the Brillouin zone) from the general much larger background.

We calculated the behavior of electrons in a periodic lattice we used, in Section 4.4 with constant potential with time. But when we treat electrons interacting with light , then alternating electric fields of the light perturbs the potential fields of the lattice periodically

$$V = V_0 + V'$$

Unperturbed potential energy

$$E = A \cos \omega t$$ **Plane polarized light** $$V' = eEx = eA\cos(\omega t)\cdot x$$

$$V = V_0 + eAx \cos \omega t$$

Put this potential energy to the Schrodinger Equation

$$\nabla^2 \Psi - \frac{2m}{\hbar^2}(V_0 + eAx \cos \omega t)\Psi - \frac{2im}{\hbar}\frac{\partial \Psi}{\partial t} = 0$$

12.4 Dispersion

$$P = Nex$$ **Classical Polarization** ➡ $$P = Ne \int x \Psi \Psi^* d\tau$$ **Quantum mechanical consideration**

Using above relations , We can obtain

$$\varepsilon_1 = n^2 - k^2 = 1 + \frac{Ne^2 A}{\varepsilon_0 \pi \hbar} \sum a_{ni}^2 \frac{v_{ni}}{v_{ni}^2 - v^2}$$

Sought-after relation for the optical properties of solids, obtained by wave mechanics

$$f_i = \frac{4\pi m}{\hbar} a_{ni}^2 v_{ni}$$ **Oscillator strength**

Part III Optical Properties of Materials

13.1.1 Karmers-Kronig Analysis (Dispersion Relations)

A relationship between real and imaginary term of any complex function, which enables one to calculate one component of a complex quantity if the other one is known: phase jump δ'(between the reflected and incident ray) from the reflectivity, *R*, which was measured at a given frequency, ν :

Kramers-Kronig relation

$$\delta'(v_x) = \frac{1}{\pi}\int_0^\infty \frac{d\ln\rho}{dv}\ln\left|\frac{v+v_x}{v-v_x}\right|dv$$

$$\rho = \sqrt{R} = \sqrt{\frac{I_R}{I_0}}$$

$$n = \frac{1-\rho^2}{1+\rho^2+2\rho\cos\delta'} \qquad k = \frac{2\rho\sin\delta'}{1+\rho^2+2\rho\cos\delta'}$$

13.1.2 Spectroscopic Ellipsometry
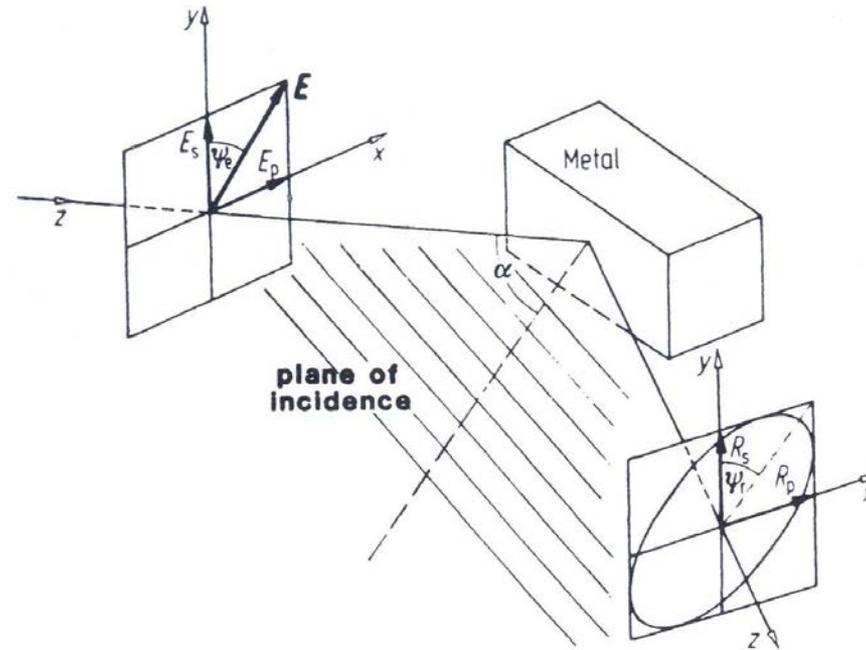
Figure 13.1. Reflection of plane-polarized light on a metal surface. (*Note*: In the figure $\mathcal{E}_{Rp} \equiv R_p$ and $\mathcal{E}_{Rs} \equiv R_s$.)

If a plane-polarized light impinges under an angle α on a metal, the reflected light is generally elliptically polarized. The analysis of this elliptically polarized light yields two parameters, the **azimuth** and the **phase difference**, from which the optical properties are calculated.
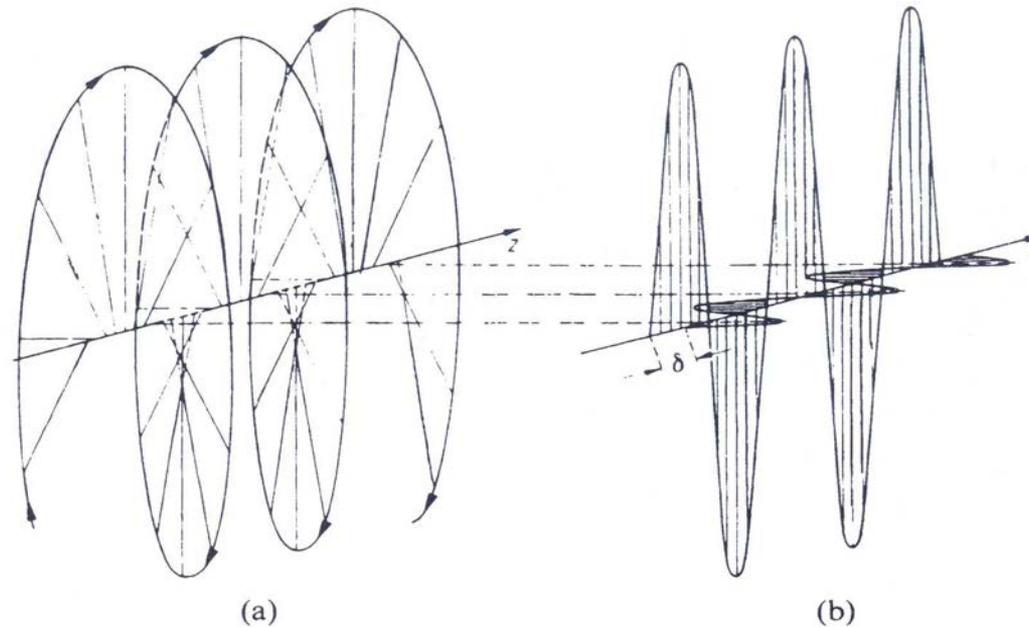
Figure 13.2. (a) Elliptically polarized light and (b) decomposition of elliptically polarized light into two mutually perpendicular plane-polarized waves with phase difference δ. Adapted from R.W. Pohl, *Optik und Atomphysik*. Springer-Verlag, Berlin (1958).

The tip of the light vector moves along a continuous screw, having the direction of propagation as an axis. Elliptically polarized light can be thought of as composed of two mutually perpendicular, plane-polarized waves, having a phase difference δ between them.
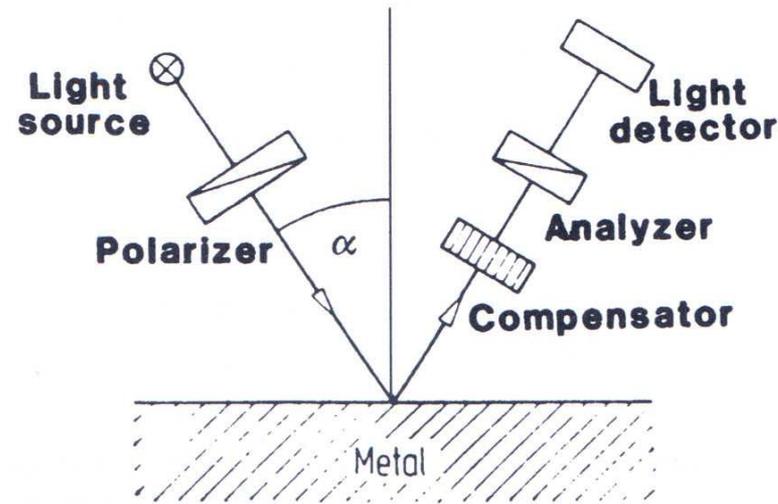
Figure 13.3. Schematic of an **ellipsometer** (polarizer and analyzer are identical devices).

For the actual measurement of ψ_r (the azimuth of reflected light) and δ (the phase difference), one needs two polarizers consisting of a birefringent material, which allows only plane-polarized light to pass, and a compensator also consisting of birefringent material, which allows one to measure the phase difference δ.
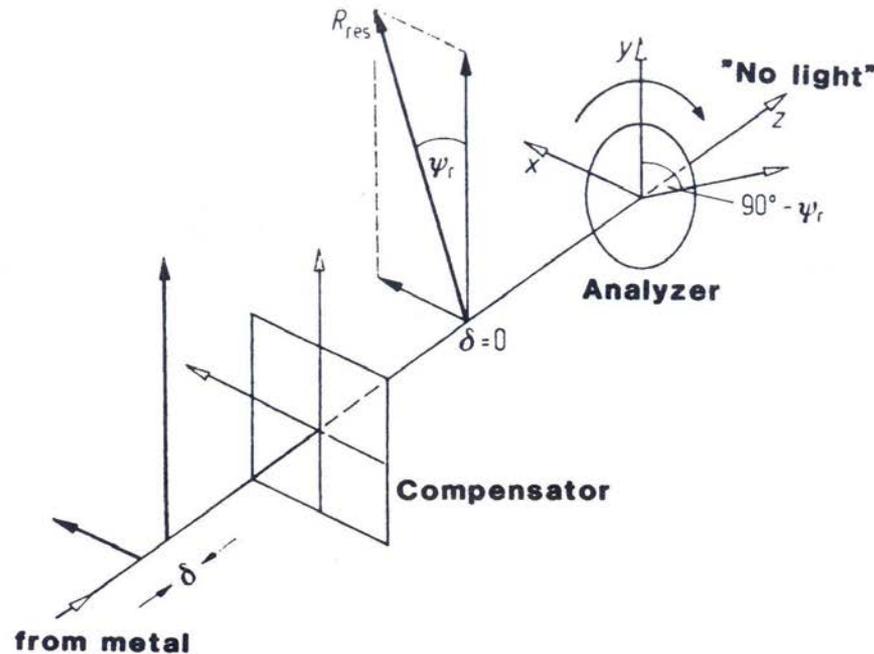
Figure 13.4. Vector diagram of light reflected from a metal surface. The vectors having solid arrowheads give the vibrational direction and magnitude of the light.

The light reflected from a metal is represented by two light vectors pointing in the *x*- and *y*- directions. Are measured by simultaneously altering the thickness of the compensator and tuning the analyzer until no light leaves the analyzer.

$$n^2 = \frac{1}{2}\left[\sqrt{(a^2 - b^2 + \sin^2 \alpha)^2 4a^2 b^2} + a^2 - b^2 + \sin^2 \alpha\right]$$

$$k^2 = \frac{1}{2}\left[\sqrt{(a^2 - b^2 + \sin^2 \alpha)^2 4a^2 b^2} + a^2 - b^2 + \sin^2 \alpha\right]$$

$$a = \frac{\sin \alpha \tan \alpha \cos 2\psi_r}{1 - \cos \delta \sin 2\psi_r} \qquad b = -a \sin \delta \tan 2\psi_r$$

$$\varepsilon_1 = n^2 - k^2 = \sin^2 \alpha\left[1 + \frac{\tan^2 \alpha(\cos^2 2\psi_r - \sin^2 2\psi_r \sin^2 \delta)}{(1 - \sin 2\psi_r \cos \delta)^2}\right]$$

$$\varepsilon_2 = 2nk = -\frac{\sin 4\psi_r \sin \delta \tan^2 \alpha \sin^2 \alpha}{(1 - \sin 2\psi_r \cos \delta)^2}$$

13.1.3 Differential Reflectometry

A differential reflectogram allows the direct measurement of the energies that electrons absorb from photons as they are raised into higher allowed energy states.

The differential reflectometer measures the normalized difference between the reflectivities of two similar specimens which are mounted side by side. (Fig. 13.5)

It belongs to a family of techniques, called modulation spectroscopy, in which the derivative of the unperturbed reflectivity (or ε_2) with respect to an external parameter is measured. (Fig. 13.6)

13.2.1 Reflection Spectra

The spectral dependence of the optical properties of metals

- Light interacts with a certain number of free electrons and a certain number of classical harmonic oscillators, or equivalently, by intra-band and inter-band transition
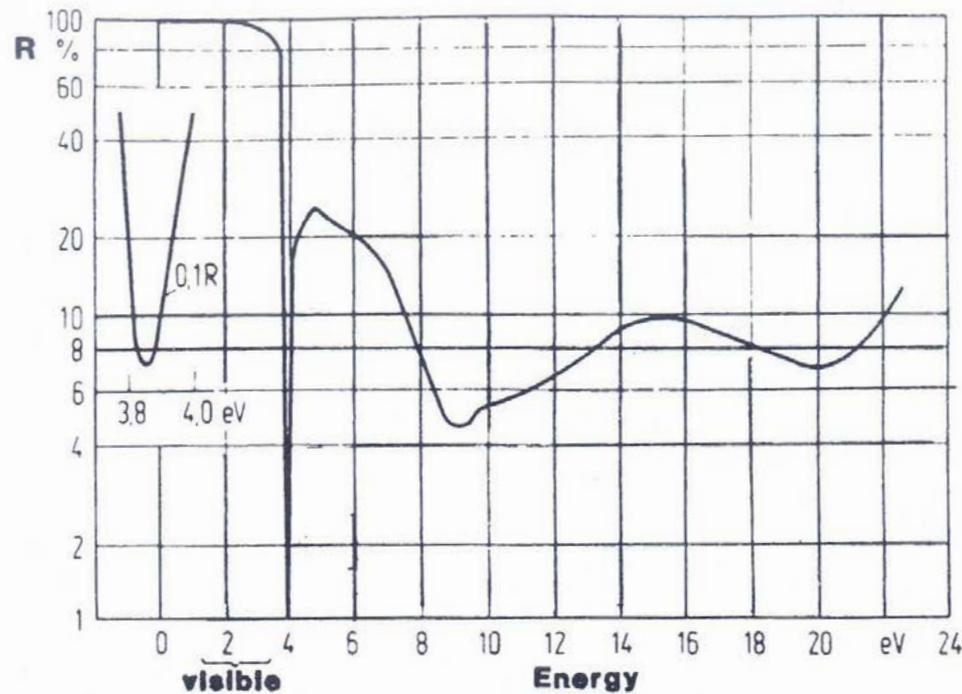
Figure 13.7. Reflectivity spectrum for silver. Adapted from H. Ehrenreich et al., *IEEE Spectrum* **2**, 162 (1965). © 1965 IEEE.
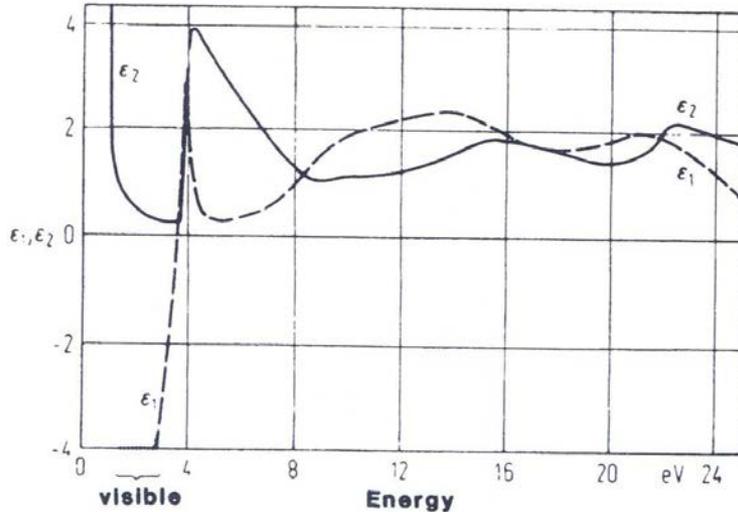
For Silver

Figure 13.8. Spectral dependence of ε_1 and ε_2 for silver. ε_1 and ε_2 were obtained from Fig. 13.7 by a Kramers–Kronig analysis. Adapted from H. Ehrenreich et al., *IEEE Spectrum* **2**, 162 (1965). © 1965 IEEE.
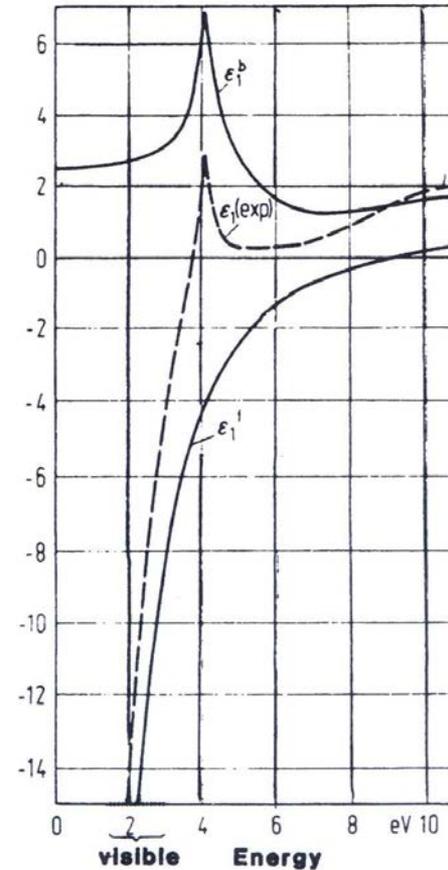
Figure 13.9. Separation of ε_1 for silver into ε_1^f (free electrons) and ε_1^b (bound electrons). Adapted from H. Ehrenreich et al., *IEEE Spectrum* **2**, 162 (1965). © 1965 IEEE.

For $E < 3.8\ eV$: the spectral dependence of ε_1 and ε_2 have the characteristic curve shapes for free electrons
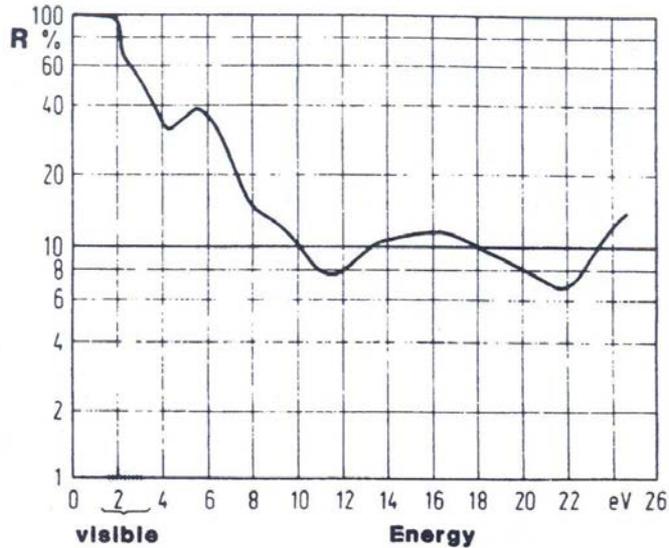
For Copper

Figure 13.10. Reflectivity spectrum for copper. Adapted from H. Ehrenreich et al., *IEEE Spectrum* **2**, 162 (1965). © 1965 IEEE.
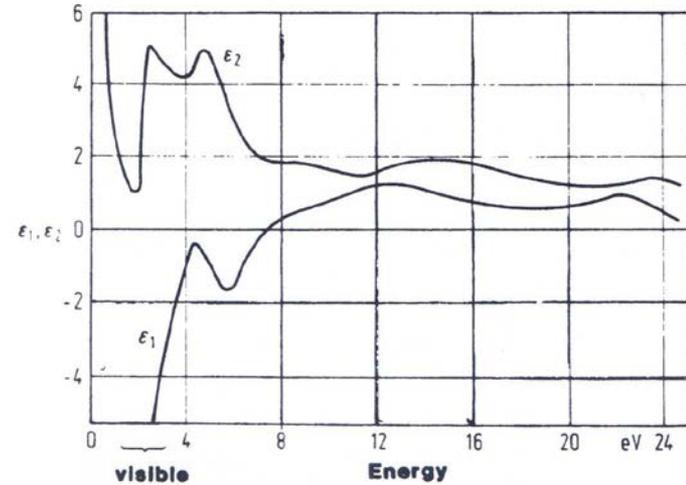
Figure 13.11. Spectral dependence of ε_1 and ε_2 for copper. ε_1 and ε_2 were obtained from Fig. 13.10 by a Kramers–Kronig analysis. Adapted from H. Ehrenreich et al., *IEEE Spectrum* **2**, 162 (1965). © 1965 IEEE.

Copper possesses an absorption band in the visible spectrum, which is responsible for the characteristic color of copper.
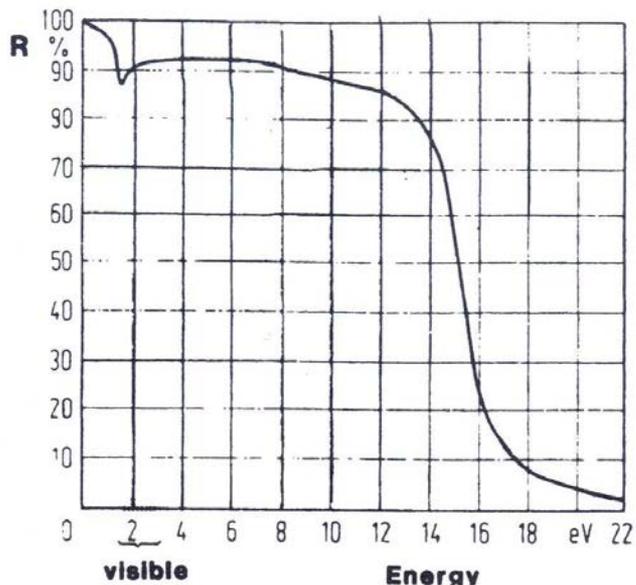
For Aluminum

Figure 13.12. Reflection spectrum for aluminum. Adapted from H. Ehrenreich et al., *IEEE Spectrum* **2**, 162 (1965). © 1965 IEEE.
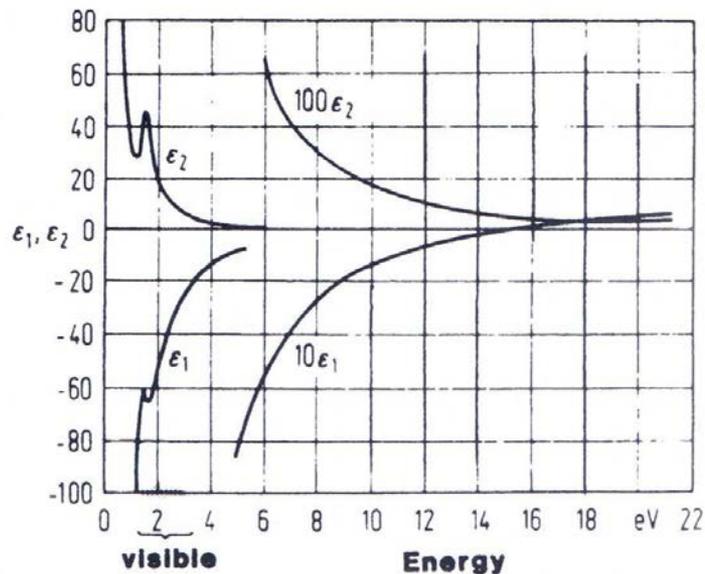
Figure 13.13. Spectral dependence of ε_1 and ε_2 for aluminum. Adapted from H Ehrenreich et al., *IEEE Spectrum* **2**, 162 (1965). © 1965 IEEE.

"Free electron-like behavior"

13.2.2 Plasma Oscillations

Plasma : excited by light of proper photon energy to collectively perform fluid-like oscillations

At plasma frequency

$$\hat{\varepsilon} = \varepsilon_1 - i\varepsilon_2 = 0$$

$$\frac{1}{\hat{\varepsilon}} = \frac{1}{\varepsilon_1 - i\varepsilon_2} = \frac{\varepsilon_1 + i\varepsilon_2}{\varepsilon_1^2 + \varepsilon_2^2} = \frac{\varepsilon_1}{\varepsilon_1^2 - \varepsilon_2^2} + i\frac{\varepsilon_2}{\varepsilon_1^2 + \varepsilon_2^2}$$

$$\mathrm{Im}\frac{1}{\hat{\varepsilon}} = \frac{\varepsilon_2}{\varepsilon_1^2 + \varepsilon_2^2}$$ **Energy loss function**
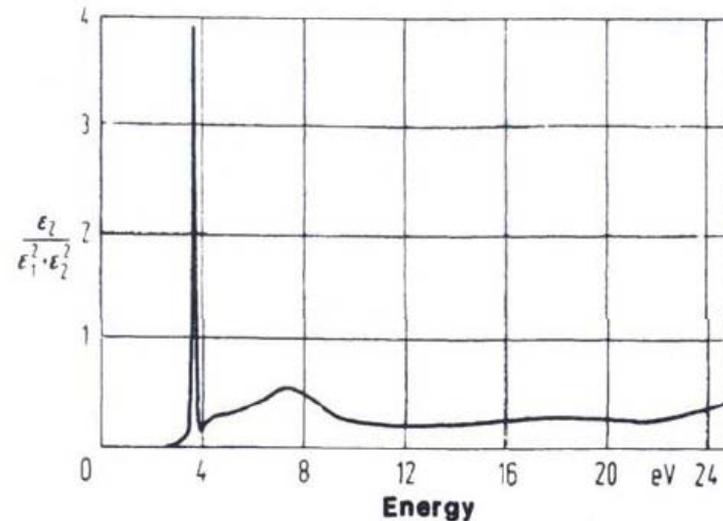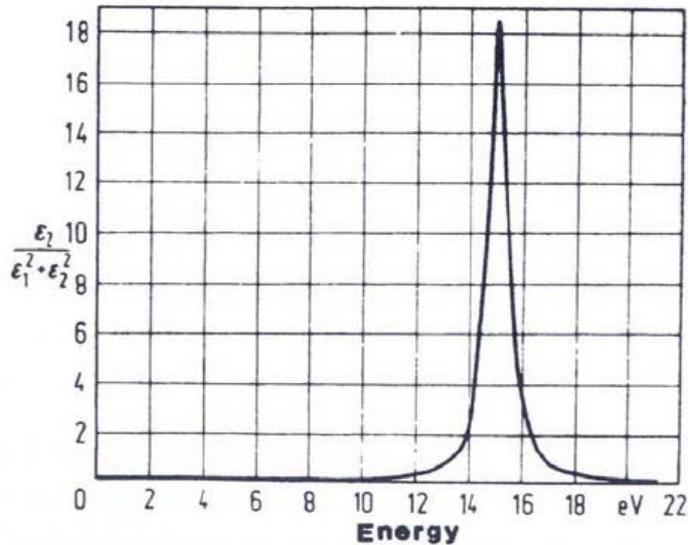
Figure 13.14. Energy loss function for aluminum. Adapted from H. Ehrenreich et al., *IEEE Spectrum* **2**, 162 (1965). © 1965 IEEE.

Figure 13.15. Energy loss function for silver. Adapted from H. Ehrenreich et al., *IEEE Spectrum* **2**, 162 (1965). © 1965 IEEE.

N.F. **Mott's suggestion** "when a small amount of metal A is added to a metal B, the Fermi energy would simply assume an average value, while leaving the electron bands of the solvent intact", called "rigid-band model". -> needed some modification.

- Cu-Zn

Fig 13.16 : a series of differential reflectograms from which the energies for inter-band transitions, E_T can be taken
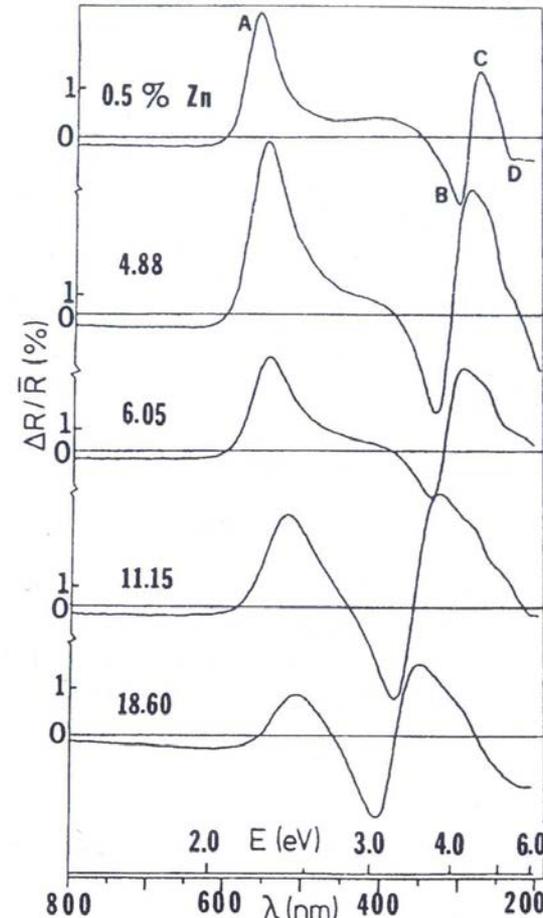
Figure 13.16. Experimental differential reflectograms for various copper–zinc alloys. The parameter on the curves is the average zinc concentration of the two alloys in at.%. The curve marked 0.5%, e.g., resulted by scanning the light beam between pure copper and a Cu–1% Zn alloy. Peaks A and D are designated as ε_2-type structures (Fig. 11.10) whereas features B and C belong to an ε_1-type structure (Fig. 11.9). From R.J. Nastasi-Andrews and R.E. Hummel, *Phys. Rev. B* **16**, 4314 (1977).

Figure 13.17. Threshold energies, E_T, for interband transitions for various copper-based alloys as a function of solute content. The E_T values are taken from differential reflectograms similar to those shown in Fig. 13.16. The rigid band line (R.B.) for Cu–Zn is added for comparison. From R.J. Nastasi-Andrews and R.E. Hummel, *Phys. Rev. B* **16**, 4314 (1977).
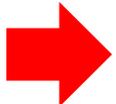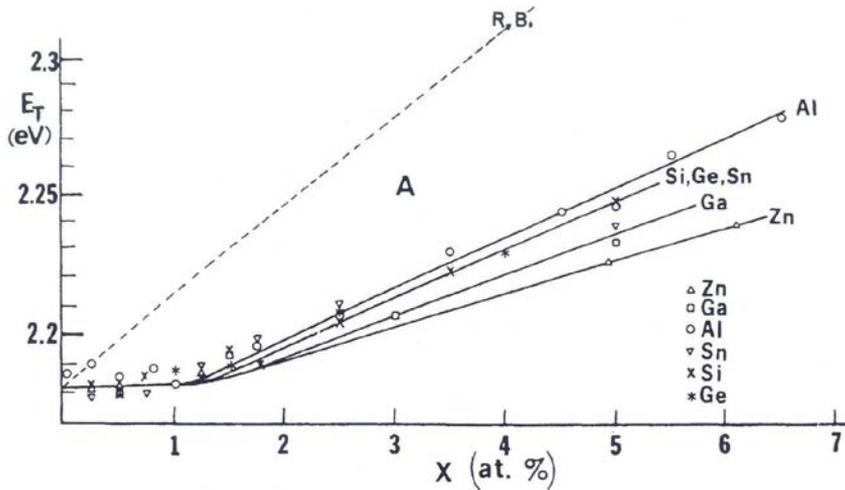
A linear increase in E_T with increasing X is observed

Schematic band structure near L for copper (solid lines), and an assumed dilute copper-based alloy (dashed lines)
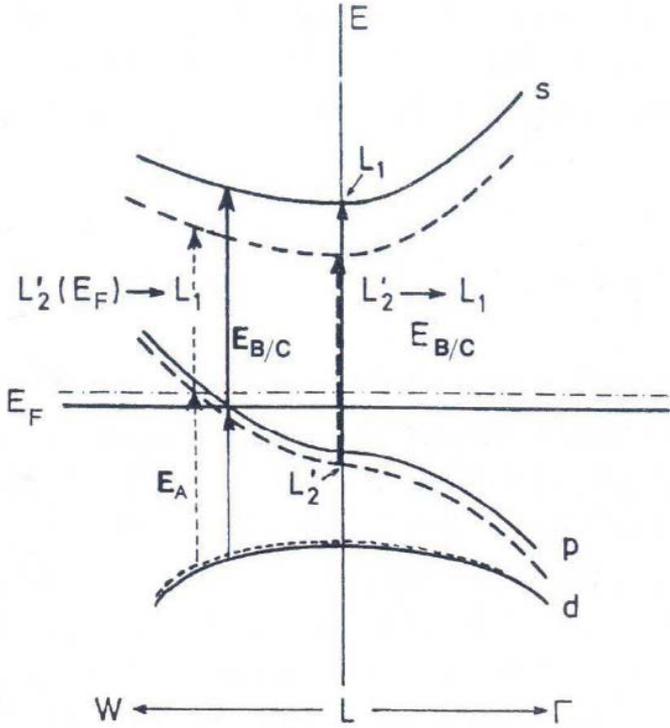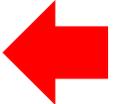
Figure 13.18. Schematic band structure near L for copper (solid lines) and an assumed dilute copper-based alloy (dashed lines). Compare with Figs. 12.3 and 5.22.

(In Sec. 7.5.3, resistivity decreases when solute atoms of an alloy are periodically arranged) The ordering has an effect on the electronic structure and hence on the optical properties of alloys
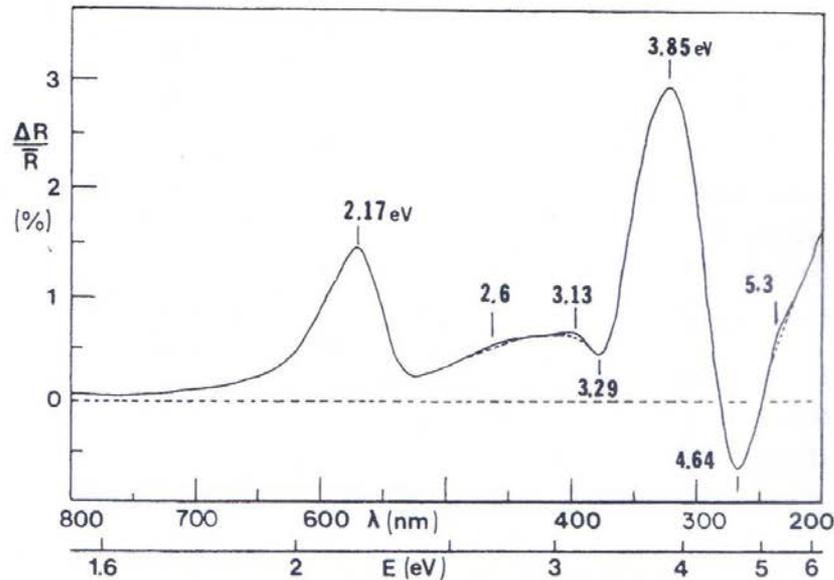
Figure 13.20. Differential reflectogram of (long-range) ordered versus disordered Cu_3Au. From R.E. Hummel, *Phys. Stat. Sol.* (a) **76**, 11 (1983).

13.4 Ordering

Short-range ordering shows comparatively smaller effects than long-range ordering
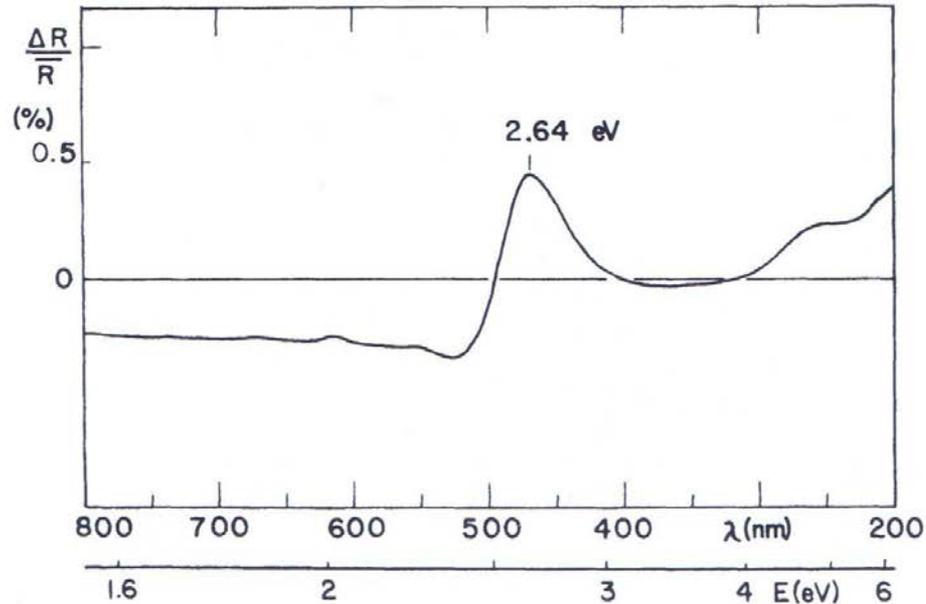
Figure 13.22. Differential reflectogram of (short-range) ordered versus disordered Cu–17 at.% Al. From J.B. Andrews, R.J. Andrews, and R.E. Hummel, *Phys. Rev. B* **22**, 1837 (1980).

"Electrochemical corrosion of copper in an aqueous solution"

- Fig 13.23 : a series of differential reflectograms demonstrating the evolution of Cu_2O on a copper substrate
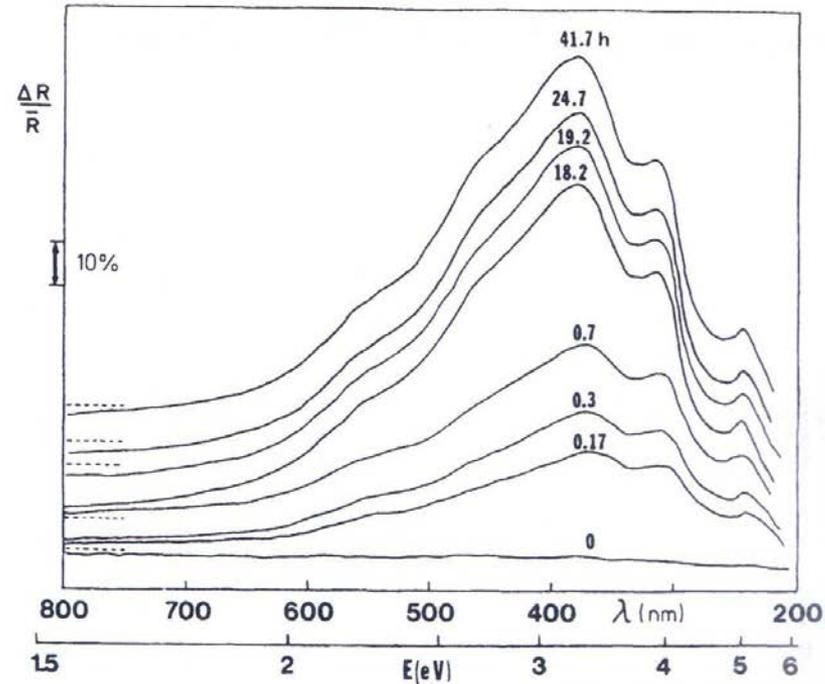
Figure 13.23. Differential reflectograms depicting the *in situ* evolution of Cu_2O on a copper substrate in a buffered electrolyte of pH 9. One sample half was held potentiostatically at -200 mV (SCE) for various times, the other at the protective potential (-500 mV (SCE)). From R.E. Hummel, *Phys. Stat. Sol. (a)* **76**, 11 (1983).

13.6 Semiconductors

- The optical behavior of an intrinsic semiconductor is similar to that of an insulator : it is transparent in the low energy (far IR) region

- Once the energy of photons are excited from the top of the valence band to the bottom of the conduction band. The semiconductor becomes opaque like a metal (Fig 13.24)
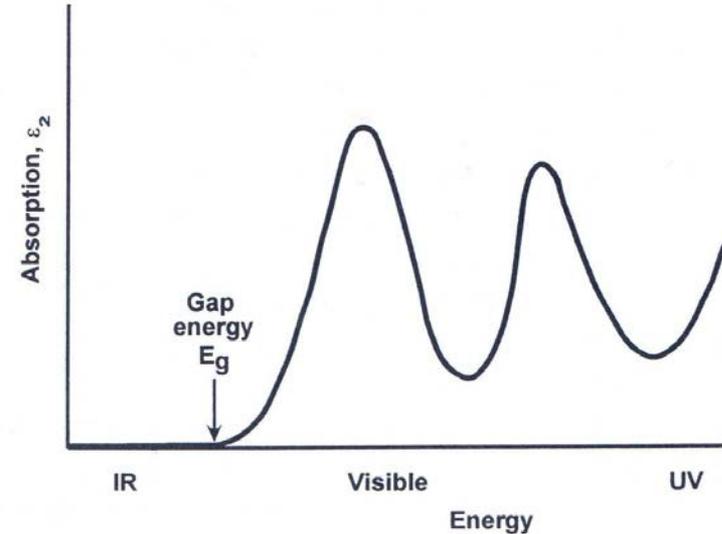
Figure 13.24. Schematic representation of the absorption spectrum of an intrinsic, direct–band gap semiconductor. The material is transparent below the gap energy and opaque above E_g.

- The onset for *inter*band transitions is thus determined by the gap energy, which characteristically values between 0.2eV and 3.5eV

13.6 Semiconductors
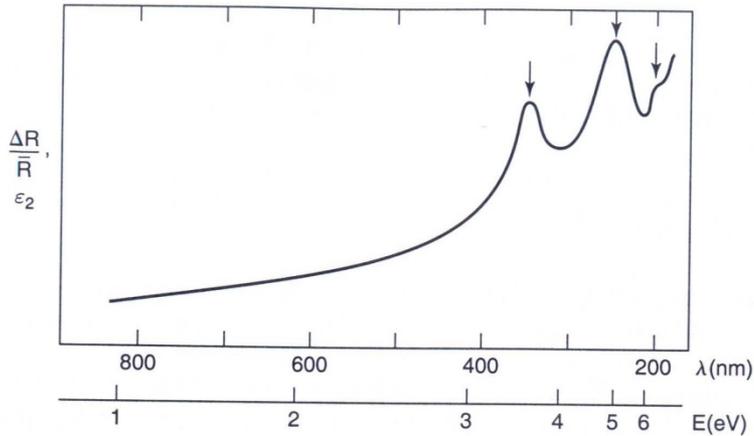
Figure 13.25. Differential reflectogram of silicon (after R.E. Hummel and W. Xi). $\Delta R/\bar{R}$ is essentially the absorption, ε_2, as explained in Section 13.1.3
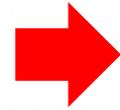
Fig 13.25

- Three distinct absorption peaks :

$L_3 \rightarrow L_1$ (3.4 eV),

Σ (4.2 eV),

$L'_3 \rightarrow$ (5.6 eV)

- These peaks are all caused by direct interband transitions in specific area of k-space

Figure 13.26. Schematic representation of direct versus indirect interband absorptions in Si. In the case of an indirect transition, a phonon needs to be additionally absorbed. Compare to Fig. 5.23 and 12.2.
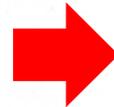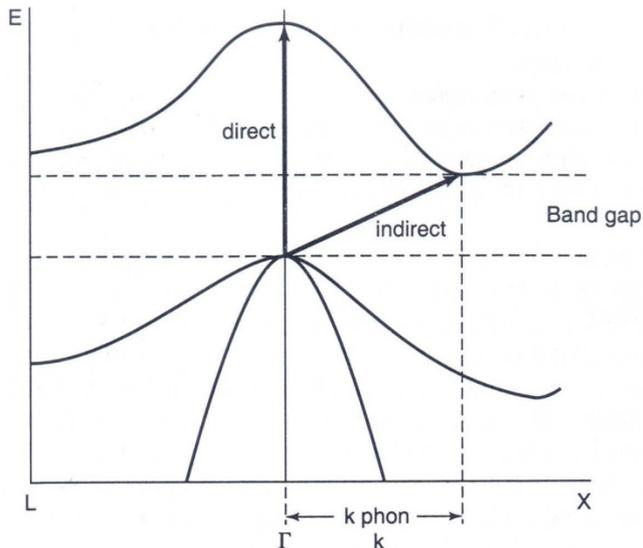
-Direct and indirect transition (Fig 13.26) : indirect transitions between the top of the valence band and the bottom of the conduction band may be possible to a limited degree provided the necessary

Momentum (wave vector k) is furnished by a photon

Photon energies slightly below the gap energy
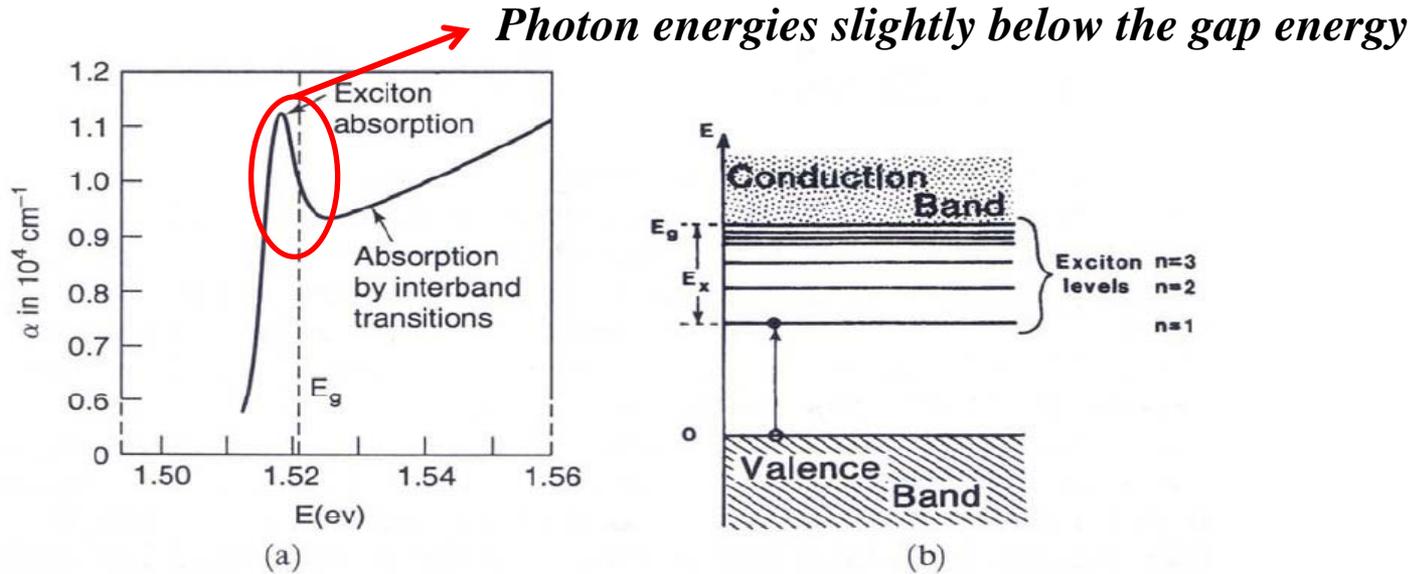
Figure 13.27. (a) Spectral dependence of the absorbance, α, (10.21a) for gallium arsenide at 21 K. Adapted from M.D. Sturge, *Phys. Rev.* **127**, 768 (1962). (b) Schematic representation of exciton energy levels and an exciton in a semiconductor (or insulator).

Exciton : a photon may exist an electron so that it remains in the vicinity of its nucleus, thus forming an electron-hole pair

$$E_x = -\frac{m^* e^4}{(4\pi\varepsilon_0)^2 2n^2 \hbar^2 \varepsilon^2} \qquad \text{Exciton Level}$$

Extrinsic Semiconductor

At high temperatures , optical transitions from and to these states can take place, which also cause weak absorption peaks below the gap energy

No intraband transitions, and large gap energy ➡ **From far IR to UV region**
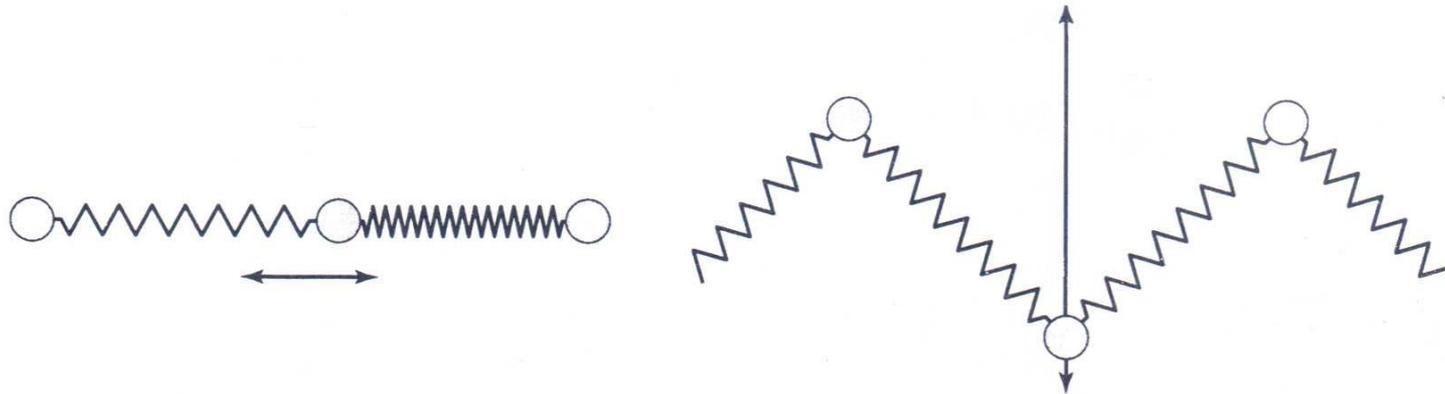
Figure 13.28. One-dimensional representations of possible vibration modes of atoms that have been excited by IR electromagnetic radiation (heat).

Excitation of phonons by photons

oscillations of atoms under the influence of light

$$m\frac{d^2x}{dt^2} + \gamma'\frac{dx}{dt} + kx = eE_0\exp(i\omega t)$$

Caused by interactions of the phonons with lattice imperfection or other things
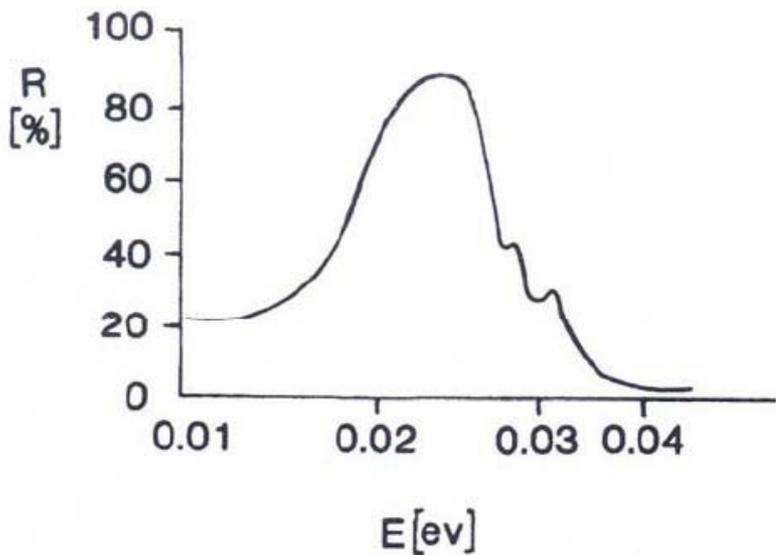
$$\omega_0 = 2k\left(\frac{1}{m_1} + \frac{1}{m_2}\right)$$

Resonance frequency for diatomic crystals

Eg) Spectral reflectivity of NaCl

Figure 13.29. Spectral reflectivity of NaCl at room temperature in the far IR region.

Eg) Spectral reflectivity of borosilicate/phosphosilicate glass
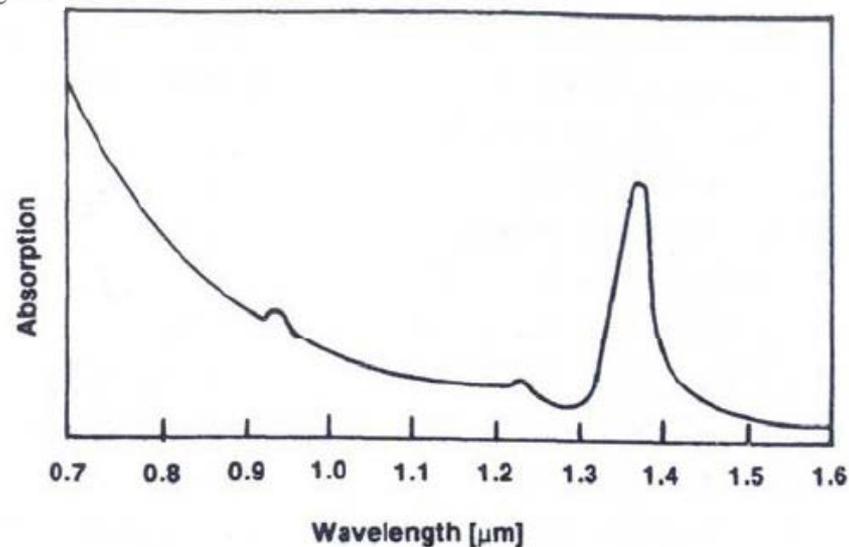
Figure 13.30. Absorption spectrum of highly purified glass for fiber-optic applications which features a phosphosilicate core surrounded by a borosilicate cladding.